Endothelin-1 modulates hippocampal and hypothalamic neuronal network activity in mouse primary dissociated cultures and brain slices

Lea Wegmann, Morris Haid, Dennis Thomassen, Olga A. Sergeeva

Article - Version of Record

Suggested Citation:
Wegmann, L., Haid, M., Thomassen, D., & Sergeeva, O. (2026). Endothelin-1 modulates hippocampal and hypothalamic neuronal network activity in mouse primary dissociated cultures and brain slices. Peptides, 198, Article 171495. https://doi.org/10.1016/j.peptides.2026.171495

Peptides 198 (2026) 171495

Contents lists available at ScienceDirect

Peptides

journal homepage: www.elsevier.com/locate/peptides

Endothelin-1 modulates hippocampal and hypothalamic neuronal network activity in mouse primary dissociated cultures and brain slices

Lea Wegmann [a,b,1,*], Morris Haid [c], Dennis Thomassen [a,b], Olga A. Sergeeva [a,b,2]

[a] Institute of Neural and Sensory Physiology, Medical Faculty & University Hospital, Heinrich Heine University Düsseldorf, Düsseldorf 40225, Germany
[b] Institute of Clinical Neurosciences and Medical Psychology, Medical Faculty & University Hospital, Heinrich Heine University Düsseldorf, Düsseldorf 40225, Germany
[c] Cécile and Oskar Vogt Institute for Brain Research, Medical Faculty & University Hospital, Heinrich Heine University Düsseldorf, Düsseldorf 40225, Germany

ARTICLE INFO

Keywords:
Endothelin-1
Endothelin receptors
Histaminergic neurons
Tuberomammillary nucleus
Hippocampus
Microelectrode Array
Patch-clamp

ABSTRACT

Endothelin-1 (ET-1) is known not only as a vasoconstrictor, but also as a neuromodulator. It can reset the circadian clock and we hypothesized that it modulates neuronal excitability and network activity in histaminergic neurons (HN). HN, located in the tuberomammillary nucleus (TMN) of the caudal hypothalamus (cHPT), fire spontaneously during waking and promote arousal. Previous studies have shown that ET-1 reduces firing frequency of hippocampal pyramidal neurons, whereas its effects on electrophysiological properties of HN remain unknown. We now studied the expression of ET-receptors (ET_A and ET_B) in the hippocampus (HPC) and caudal hypothalamus by single-cell RT-PCR and qPCR. The responses to ET-1 were studied in HN and dentate gyrus granule cells (DGgc) of brain slices using patch-clamp recordings and primary cultures of cHPT and HPC using Microelectrode Arrays (MEAs).

ET-1 significantly decreased firing frequency in HPC and increased it in cHPT cultures with prevailing inhibition of individual MEA channels in HPC and excitation in cHPT. Neuronal synchrony and bursting were significantly increased in cHPT. Relative to HPC, cHPT displayed higher expression of ET_B. In brain slices, ET-1 induced a delayed bosentan-sensitive increase in HN and decrease in DGgc firing frequency. HN expressed ET_B (15 of 22 HN) and ET_A (4 of 15 ET_B positive HN), whereas only ET_B was expressed in 50% of DGgc.

We conclude that ET-1 differentially modulates cHPT and HPC. By exciting HN and synchronizing neuronal network activity in cHPT, ET-1 may contribute to cellular and circuit-level mechanisms in the regulation of arousal and wakefulness.

1. Introduction

Endothelin-1 (ET-1) is a 21-amino acid peptide that binds to the G-protein-coupled ET-receptors (ET_A and ET_B). Initially described in 1988 by Yanagisawa and colleagues as a potent vasoconstrictor synthesized by vascular endothelial cells [1], ET-1 has continuously attracted the attention of scientists working in different fields in the following decades [2], including neuroscientists, who demonstrated an expression of ET-1 and its receptors in the brain and a role of ET-1 as a neuromodulator in circuits processing stress, pain and anxiety [3–5]. ET_A and ET_B represent pharmacological targets for the treatment of pulmonary hypertension and other diseases, with dual-receptor antagonist bosentan becoming the first clinically approved drug targeting ET-receptors in 2001 [2]. Recent clinical trials with next-generation ligands explore the potential of this target for the treatment of neurological disorders such as ischemic stroke, encouraging more research into mechanisms of ET-1 action in the brain [6].

The ET-1 peptide is known to be involved in the regulation of the circadian clock [7], exhibiting a circadian rhythm in its expression in several tissues that peaks during wakefulness [8]. It is also proposed to synchronize the circadian clock [9,10]. This suggests that ET-1 may be involved in neuronal circuits of arousal regulation. Histaminergic

* Correspondence to: Institute of Neural and Sensory Physiology, Institute of Clinical Neurosciences and Medical Psychology, Medical Faculty & University Hospital, Heinrich Heine University, Düsseldorf D – 40225, Germany.
E-mail addresses: lea.wegmann@hhu.de (L. Wegmann), morris.haid@hhu.de (M. Haid), dennis_thomassen@web.de (D. Thomassen), olga.sergeeva@hhu.de (O.A. Sergeeva).
[1] ORCID iD: 0009-0003-6639-6116
[2] ORCID iD: 0000-0002-2713-1145

https://doi.org/10.1016/j.peptides.2026.171495
Received 3 March 2026; Received in revised form 17 May 2026; Accepted 25 May 2026
Available online 27 May 2026

neurons (HN) located in the tuberomammillary nucleus (TMN) of the caudal hypothalamus (cHPT) fire spontaneously during waking and are silent during slow-wave sleep [11]. They project to various brain regions and integrate sensory inputs with the inputs from other ascending reticular activating system (ARAS) neurons, adjusting behavior to a changing environment [11]. HN are sensitive to many peptides which are known to stabilize arousal, such as orexin [12], thyrotropin-releasing hormone (TRH) [13] and substance P [14]. However, effects of ET-1 on electrophysiological properties of HN and the expression of ET-receptors by HN remain unknown.

In the hypothalamus, an expression of ET-1 [15,16], its receptors and endothelin converting enzyme 1 (ECE-1), which cleaves "big endothelin-1" into biologically active ET-1 [17], is observed, indicating a possible peptide function as a neurotransmitter. Studies on effects of ET-1 on brain neurons are limited and many report bidirectional effects of this peptide or ET-receptor agonists on neuronal activity [18,19]. Confounding effects of vasoconstriction and tissue movements have been described in some electrophysiological studies [20]. Among the few electrophysiological studies investigating ET-1 effects, an increase [21,22], a decrease [3–5] or no change [23] of neuronal activity have been described in different brain regions. In the hippocampus, ET-1 was shown to influence synaptic plasticity by blocking the induction of long-term potentiation (LTP) of synaptic transmission and facilitating the induction of heterosynaptic long-term depression (LTD) [24]. ET-1 reduces firing frequency of pyramidal neurons with predominant expression of ET-1 and its receptors in pyramidal neurons of the CA1 region [3]. Because of the well-described modulation of hippocampal neuronal activity by ET-1 [3,24] and known ET-receptor expression in individual hippocampal principal cells (e.g. in "Hipposeq" single-cell RNA sequencing database [25]), we selected the hippocampus as a reference region to study effects of ET-1 on HN of TMN.

Given the reported circadian role of ET-1 and the expression of ECE-1, ET-1 and receptors in the hypothalamus, we hypothesized that ET-1 influences the electrophysiological properties of histaminergic neurons and neuronal network activity in cellular circuits relevant to arousal regulation.

To study the responses to ET-1 application, we performed now electrophysiology using patch-clamp recordings in identified HN and dentate gyrus granule cells (DGgc) of mouse brain slices and Microelectrode Array (MEA) recordings of hippocampal (HPC) and caudal hypothalamic (cHPT) cultures. ET-receptor expression was studied using single-cell RT-PCR in HN and DGgc and qPCR in hippocampal and caudal hypothalamic tissues.

2. Materials and methods

2.1. Animals

For Microelectrode Array experiments and patch-clamp recordings, juvenile and adult female and male mice with a C57BL/6 genetic background were sacrificed. Specifically, mice expressing the fluorescent Tomato protein controlled by the histidine decarboxylase promotor Tmt-HDC, their parent lines (HDC-Cre and Rosa26-lox-STOP-lox-Tomato (Tmt)) and other Cre-lines were used. Animals were held under specific pathogen-free conditions with free access to water and food. A 12/12 h dark/light cycle (with light on at 7 a.m.) was maintained at a temperature of 18–22 °C and 55% humidity. All procedures were performed in compliance with the directive 2010/63/EU of the European parliament and the German animal protection law "Tierschutzgesetz". Permission was granted by the local authorities (LANUV NRW: Landesamt für Umwelt, Natur und Verbraucherschutz Nordrhein Westfalen, Bezirksregierung Düsseldorf; AZ 19/63–102_6 from 18/12/2023). All efforts were made to minimize the number of animals and their suffering.

2.2. Primary dissociated cell culture

We prepared primary dissociated cell cultures from the whole hippocampus and caudal hypothalamus in a parallel fashion as previously described in [26]. A total of 24 independent platings used for MEA recordings were made from mice aged 0–4 days (n = 2–8 per plating). After dissociation, 60 µL of cell suspension in medium containing minimal essential medium (MEM, Gibco Cat. (catalogue) No. 11090081) was plated on Microelectrode Arrays (MEAs). After four hours of incubation (5% CO_2, 95% air, 98% relative humidity, 37 °C temperature) we added 1.6 mL of growth medium containing 2% B27 plus (Invitrogen, Cat. No. A35828) and 1% Penicillin-Streptomycin (Sigma-Aldrich, Cat. No. P4458) and either Neurobasal Plus Medium (NBMplus, Gibco, Cat. No. A3582901) or MEM. Exchange of culture medium was performed once per week. MEA recordings were performed between 5 and 33 days *in vitro*.

2.3. Microelectrode Array (MEA) recordings

60-electrode Microelectrode Arrays (MEAs) with planar Ti/TiN-microelectrodes were used for recordings (30 µm diameter, 200 µm spacing, Cat. No. 890953, Multi Channel Systems, Reutlingen, Germany). Prior to plating of cells, MEAs were coated with polyethylenimine (Sigma-Aldrich, Cat. No. P3143). Recording temperature was maintained at 33–37 °C. We adjusted the pH of our recording medium to 7.4, which contained (in mM): NaCl (150), KCl (3.7), $CaCl_2$ (2.0), $MgCl_2$ (0.5), HEPES (10) and glucose (10). The recording medium HEPES-buffered solution (HBS) replaced the growth medium before an accommodation period of 10–20 min. The agonist was applied for 5 min after a 7-minute baseline period in HBS. Agonist application was followed by a 7-minute washout period. In case of application of agonist in the presence of an antagonist, the recording comprised of 7 min in HBS, 7 min antagonist application, 5 min of common application (agonist and antagonist), 7 min antagonist application and a 7-minute washout period.

Extracellular potentials were recorded simultaneously from all 60 electrodes with a sampling rate set at 25 kHz, visualized and stored using the software MCRack (Multi Channel Systems, Reutlingen, Germany). Spike and burst detection was performed offline using the software SpAnNer (RESULT Medizinische Analyseverfahren, Toenisvorst, Germany). For each individual electrode, the spike detection thresholds were set to 8 standard deviations, referring to the average noise level during an initial 10% learning phase at the beginning of each recording. The spike detection algorithm was imposed with a 4 ms absolute refractory period and a maximum spike width of 2 ms. Overall synchrony of neuronal discharge was evaluated using the parameter Cohen's kappa (further called "kappa"), with higher values closer to one indicating strong synchrony and lower values closer to zero indicating weak synchrony. Kappa was calculated according to an algorithm described in detail in previous publications [27,28] with two modifications. First, only channels with at least 10 spikes during recording bins (60 s) were included in the analysis. Second, spike trains were analyzed with a bin width of 100 ms. Previous studies have shown that kappa [27,28] same as other synchrony metrics such as the global synchrony index, SPIKE-distance measure and spike time tiling coefficient (STTC) [29] are all suitable to detect an increase in network synchrony induced by bicuculline ($GABA_A$-receptor antagonist).

Spontaneous spikes per minute (referred to as firing frequency: FFR or S/min) and bursts per minute (B/min) were averaged across all electrodes or separated in excited or inhibited channels by a Python-based sorting algorithm (see 2.8). FFR, B/min and kappa are presented as mean ± SEM, with n referring to the number of recordings and N to the number of independent experiments (platings).

2.4. Slice electrophysiology

30 mice aged 90.5 ± 16 days (14 male and 16 female) were used for patch-clamp experiments. Among them, 20 mice carried a Tmt-HDC genotype. Mice were sacrificed between 9 and 11 a.m. (for details see [14]). We prepared two to three 250 μm coronal brain slices at the level of TMN from each mouse with a tissue slicer (HR2, Sigmann Elektronik, Germany) as in our previous study [26]. For cutting and dissection, the tissue was placed in ice-cold artificial cerebrospinal fluid (ACSF) composed of (in mM): Sucrose (202), D-Glucose (12), $NaHCO_3$ (26), KCl (3.75), NaH_2PO_4 (1.25), $MgSO_4$ (1.3) and $CaCl_2$ (2). ACSF was saturated with carbogen (5% CO_2/95% O_2), maintaining the pH at 7.4. Slices were transferred to an incubation glass and ACSF composition was changed to contain 125 mM NaCl instead of 202 mM sucrose for further incubation. The next 1–7 h before recording, the slices were incubated at room temperature (~22 °C). About 30 min before the start of recordings the slices were transferred to a heated chamber (32 °C). In the recording chamber the slices were perfused with calcium-free ACSF (CF-ACSF) at 2 mL/min. In CF-ACSF, the $MgSO_4$ concentration was increased to 2.6 mM, Ca^{2+} removed and EGTA (0.5 mM) included.

We recorded signals in cell-attached voltage clamp mode using the Multiclamp 700B amplifier (Molecular Devices, San Jose, USA) with patch pipettes made of 1.5 mm (OD) borosilicate glass (Science Products GmbH, Hofheim, Germany) filled with ACSF (resistance 4.5 – 6 MΩ) using a horizontal microelectrode puller (P-87, Sutter Instrument, Novato, USA). Using infrared light and differential interference contrast (IR-DIC) optics (Axioscope 2 FS, Zeiss, Oberkochem, Germany), cells were visualized and approached. Image detection was performed using an infrared-sensitive video camera (Newvicon C2400, Hamamatsu, Hamamatsu City, Japan). HN were identified genetically (in Tmt-HDC mice by red fluorescence as in [30]) and pharmacologically by the application of H3-receptor agonist (R)(−)-α-Methylhistamine (RAMH, 2 μM), inducing an inhibition and by H3-receptor antagonist clobenpropit (20 μM), inducing an excitation (see supplementary Fig. 1)

Using the pCLAMP 10 software (Axon Instruments, Foster City, USA), signals were analyzed, filtered between 0.5 and 10 kHz and sampled at 20 kHz. Manual analysis and detection of extracellular action potentials were performed with the software MiniAnalysis 6.0.1 (Synaptosoft Inc., Fort Lee, USA), which works with the old format of axon binary files (abf). pCLAMP 10 generates abfx files and their manual conversion into abf files is a time-consuming process. Therefore, for automatic batch conversion of abfx files, the software "mhaid_abfconverter" was written in Python (≥3.10), using pyABF (Harden, SW (2022), version 2.3.8) internally. Firing frequency was calculated from interevent intervals in 60 s bins. Drugs were applied for 7 min after 7 min of baseline recording. In experiments with common application of agonist and antagonist (7 min), the antagonist was pre-applied for 7 min and continued to be applied for 9 min after agonist withdrawal. As Yamamoto et al. [18] have shown that repeated endothelin applications in hypothalamic neurons yield good responses, we decided to perform in all recorded cells the first application of ET-1 in the presence of bosentan and the second (control) application of ET-1 was performed after 20–25 min from the first application. Data are presented as a change in firing frequency (Hz) relative to a 7-minute baseline period, with n referring to the number of recorded cells and N to the number of independent experiments (mice).

2.5. Semiquantitative PCR (qPCR)

We used the same protocols for tissue dissection, mRNA purification (Dynabeads™ mRNA DIRECT™ Micro Kit, Thermo Fisher Scientific, Cat. No. 61021), cDNA synthesis (First Strand cDNA synthesis kit, Cytiva via VWR, Cat. No. 27926101) and Real-Time PCR as in our previous study [26]. In brief, we amplified cDNAs derived from the whole caudal hypothalamus (cHPT) or hippocampus (HPC), both dissected from coronal slices (0.5–1 mm thick) cut at the level of the tuberomammillary nucleus (TMN) between 10 and 11 a.m. HPC and cHPT tissues were dissected and analyzed in parallel fashion in 8 male and 11 female mice aged from 100 to 329 days (181 ± 16 days, n = 19). Obtained cDNA samples were diluted by adding 15 μL water to 1 μL of cDNA, and the exact concentration of nucleic acid was measured in each sample on Nanodrop™ 2000c (PeqLab, Thermo Fisher Scientific). Amplifications were performed in the Applied Biosystems™ StepOnePlus™ real-time PCR machine using the SYBR™ Green PCR master mix kit (Applied Biosystems via Thermo Fisher Scientific, Cat. No. 4309155). Reactions were performed in MicroAmp™ optical 96-well plates in a total volume of 10 μl containing the final concentration of PCR Master mix, primers (see Tables 1) and 1 μL of cDNA (236 ± 5 ng, n = 38, no difference in cDNA concentration between brain regions and sexes, One-way ANOVA, $F(3,34) = 0.9$, $p = 0.45$). The following thermal protocol was performed: initial incubation at 50 °C for 2 min to activate uracil N-glycosylase, 10 min at 95 °C to inactivate the uracil N-glycosylase and activate the AmpliTaq™ Gold Polymerase, and finally 40 cycles of 15 s at 95 °C and 1 min at 60 °C. At the end of PCR cycling the heat denaturation protocol was executed. All products showed a single peak in DNA melting curves. Every sample was amplified two to five times and all reactions were carried out in duplicates, "calibrator" was present in every reaction and 13 amplifications were performed in total. The relative mRNA-level of ET_A or ET_B (in % of calibrator HPC of female mouse #1908, 207 days old) was estimated by the "$2^{-\Delta\Delta Ct}$ method" with normalization on the expression of the ribosomal protein L13A (RpL13a), where ΔCt = Ct target gene - Ct [26]. Standard curves were obtained with sequential dilutions of one cDNA sample and were found optimal for all three primer pairs: ET_A receptor, ET_B receptor and RpL13a (linear regression coefficients were > 0.95).

2.6. Single-cell RT-PCR

Coronal brain slices were prepared as for patch-clamp recordings and first incubated at room temperature for at least 2 h. 14 mice (9 males, 5 females), 16–315 (on average 52 ± 21) days old, were used for these experiments. Acutely isolated neurons were obtained by papain digestion of the tissue as previously described [13]. In brief, hippocampal or cHPT slices containing TMN were incubated with papain in crude form (0.3–0.5 mg/mL) for 30 min at 37 °C. After rinsing, ventrolateral TMN or DG were dissected under the binocular microscope and placed in Eppendorf tubes containing 50 μL of HEPES-based ACSF of the following composition (in mM): NaCl (150); KCl (3.7); $CaCl_2$ (2.0); $MgCl_2$ (2.7); HEPES (10) and glucose (10). The pH was adjusted to 7.4 with NaOH. Cells were separated by gentle pipetting and placed in the recording chamber, where selected cells were digitally photographed. Cells were approached with a patch-clamp electrode filled with the solution for intracellular recordings (in mM): KCl (130); NaCl (10); $MgCl_2$ (2); $CaCl_2$ (0.25); glucose (5); HEPES (5); EGTA (10); MgATP (5) and MgGTP (0.3); a pH of 7.2 was adjusted with KOH (1 M). After a good seal between the electrode and cellular membrane was obtained, the cytoplasm of the cell was harvested into the electrode. We expelled the pipette content (8 μL) into the Eppendorf tube with first-strand cDNA synthesis kit (First Strand cDNA synthesis kit, Cytiva via VWR, Cat. No. 27926101), mixed the sample using a vortex mixer, centrifuged it (10000 rpm, 1 min) and incubated it at 37 °C overnight. To terminate reverse transcription the samples were frozen at −80 °C. We used a two-round amplification strategy. HN and DGgc were first identified by expression of histidine decarboxylase (HDC, for primers and protocols see [31]) or PDZd2 (marker of DGgc, as in [26]). ET_A and ET_B-expression were evaluated in samples positive for HDC or PDZd2 ("PCR positive"). Amplifications were performed in a volume of 10 μL containing at maximum 15% of cDNA template. We separated the amplified products using 2.5% agarose gels stained with "GelRed™ Nucleic Acid Gel Stain" (Biotium, Fremont, CA, USA, Cat. No. 41003).

Table 1
List of primer sequences (5'-> 3') used for quantitative (Q)- or/and for single-cell RT- PCR listed in forward (sense) and reverse (antisense) orientation with (1) for the first amplification round or in the second (2) amplification round, size of expected PCR products given in base pairs (b.p.), previously published primers indicated by * [32] and ** [33].

gene	forward	reverse	Product size, b.p.
ET_A receptor (2)	CTCAAACAGCGTCGAGAAGT	TGCCAGGTTAATGCCGATGT	183
ET_A receptor (1)	CTCAAACAGCGTCGAGAAGT	ACAGCAACAGAGGCAGGACT*	270
ET_A receptor (Q)	TGCTGGTTCCCTCTTCACTT*	ACAGCAACAGAGGCAGGACT*	210
ET_B receptor (2,Q)	GAGCTGAGATGTGTAAGCTG**	GAGACCACCCAAATTAAAAC**	178
ET_B receptor (1)	GAGCTGAGATGTGTAAGCTG**	GCGGCAAGCAGAAGTAGAAA	348
RpL13a (Q)	ATGACAAGAAAAAGCGGATG	CTTTTCTGCCTGTTTCCGTA	214

2.7. Drugs

The following drugs were used for electrophysiological recordings: endothelin-1 (Sigma-Aldrich, Cat. No. E7764), bosentan (Tocris, Cat. No. 6232), (R)(−)-α-Methylhistamine dihydrochloride (RAMH, Sigma-Aldrich, Cat. No. H128), clobenpropit (Tocris, Cat. No. 11213569).

2.8. Statistical analysis

Data were analyzed using Excel and GraphPad Prism versions 5, 7.08 or 10.6.1 (La Jolla, USA).

We tested for normal distribution using the Shapiro-Wilk test. For normally distributed data, the unpaired *t*-test was used for the comparison of two groups (results reported as *t*(degrees of freedom (df)) and *p* value). In case no normal distribution was detected in at least one group, we used the non-parametric Mann-Whitney *U* test (MWT) for two groups (statistical value reported as *U*(N1,N2), where N1: number of experiments in group 1 and N2: number of experiments in group 2). For the comparison of conditions within the same recordings, a paired *t*-test (reported as *t*(df), *p* value) was used.

To detect differences in effects across multiple timepoints during the same recording (baseline, drug application and washout period) a Friedman test (presented as chi-square (df), *p* value) followed by Dunn's multiple comparisons test was used for non-normally distributed data and repeated-measures one-way ANOVA (reported as *F*(DFn, DFd) = statistical value) followed by Dunnet's multiple comparisons test for normally distributed data. Repeated-measures two-way ANOVA was used to compare response-time dependence between two conditions (male vs. female mice). Differences in effect probability were estimated using Fisher's exact probability test (FEPT) or chi-square test. Correlation was estimated using the Pearson correlation coefficient *r*. Data are presented as mean ± SEM. *P* values < 0.05 were considered statistically significant.

MEA channel-wise spike rates were extracted from SpAnNer Excel outputs and processed in a custom Python (≥3.10) pipeline leveraging pandas and SciPy. For each channel, normality of pre- and during-application rate distributions was assessed via the Shapiro–Wilk test. If both periods passed ($p > 0.05$), Levene's test determined homogeneity of variance. Depending on these assessments, the script automatically selected one of three comparison tests: unpaired *t*-test (normal & equal variance), Welch's *t*-test (normal & unequal variance) or Mann–Whitney *U* test (non-normal). A channel was deemed "responding" if any applicable test yielded $p \leq 0.06$, otherwise it was flagged as "*p*-Error" but retained for reporting. Significant channels were then classified as "excited" or "inhibited" based on whether the mean spike rate increased or decreased during application.

The baseline stability was verified by comparing the average firing rate of the first and last two minutes of the pre-application period. Channels exhibiting a change > 50% were marked "unstable" and excluded from further analysis. Finally, the script tabulates the total and percentage of invalid channels (those labeled "*p*-Error" or "unstable baseline") relative to all channels passing initial inclusion filters.

3. Results

3.1. ET-1 differentially modulates firing frequency of cultures from the hippocampus and caudal hypothalamus through ET-receptor signaling

We first examined network-wide effects of ET-1 application on primary cultures derived from HPC and cHPT. Firing frequency (FFR) measured as the total number of spikes per minute (S/min) among all MEA electrodes was significantly reduced by ET-1 in HPC (paired *t*-test, $t(8) = 5.22$, $p = 0.0008$) and increased in cHPT (paired *t*-test, $t(11) = 2.57$, $p = 0.026$) compared to water application within the same recording (Fig. 1A, B). In HPC, maximal effect was observed during the first minute of ET-1 (200 nM) application, with a reduction of FFR to 49.3 ± 8.2% of baseline (Fig. 1A, left). In cHPT, ET-1 induced excitation developed slowly and reached its maximal values after withdrawal of the peptide (Fig. 1A, right). We compared 5 min averages obtained from the application period of ET-1, ET-1 in the presence of bosentan or water (Fig. 1B). In HPC, ET-1 reduced FFR to 72 ± 6.2% of baseline (n = 9, N = 5) and increased it to 117.3 ± 17.7% in the presence of bosentan (Fig. 1B, bottom) n = 8, N = 7, MWT, $U(N1 = 8, N2 = 9) = 7$, $p = 0.004$). In cHPT, firing frequency was increased by ET-1 to 115.8 ± 8.5% of baseline (n = 17, N = 12) but reduced in the presence of bosentan to 91.7 ± 9.5% of baseline (n = 10, N = 6). The difference between responses to ET-1 200 nM alone and ET-1 200 nM in the presence of bosentan 100 μM in cHPT was significant (Fig. 1B, bottom, unpaired *t*-test, $t(25) = 1.83$, $p = 0.04$). Because bosentan 10 μM seemingly did not antagonize ET-1-responses in cHPT in our initial experiments, a concentration of 100 μM was used in all cHPT experiments shown here instead. Application of water did not change neuronal firing frequency either in HPC (103.3 ± 13.9% (n = 9, N = 5) of baseline, paired *t*-test, $t(8) = 0.47$, $p = 0.65$) or in cHPT (97.9 ± 17.4% of baseline (n = 12, N = 10), paired *t*-test, $t(11) = 0.42$, $p = 0.68$). Moreover, neither in HPC nor in cHPT, ET-1 application in the presence of bosentan differed from water control (HPC: MWT, $U(N1 = 8, N2 = 9) = 32$, $p = 0.74$; cHPT: unpaired *t*-test, $t(20) = 0.61$, $p = 0.55$). In summary, ET-1 induces an inhibition of firing frequency in the hippocampus and excitation in the caudal hypothalamus, both significantly attenuated by bosentan.

3.2. Single MEA channel analysis reveals predominant inhibition in the hippocampus and excitation in caudal hypothalamus

To investigate the neuronal heterogeneity in responsiveness to ET-1, we analyzed the activity of individual MEA channels that were responsive to ET-1 application (excitation vs. inhibition). This analysis has the advantage of a high spatial resolution and enables us to detect local effects that may be masked when averaging the activity among all MEA electrodes. Single MEA channel data show a prevailing inhibition in HPC and excitation in cHPT (Fig. 2A-D). Representative heatmaps of individual channels in two MEA recordings illustrating changes in firing frequency in HPC and cHPT during ET-1 application relative to the baseline are shown in Fig. 2D. Relative frequency change is encoded by color, with the maximal increase in frequency (excitation) in green and the maximal decrease (inhibition) in purple. Excitation in cHPT and HPC does not return to baseline during the washout period, with peak

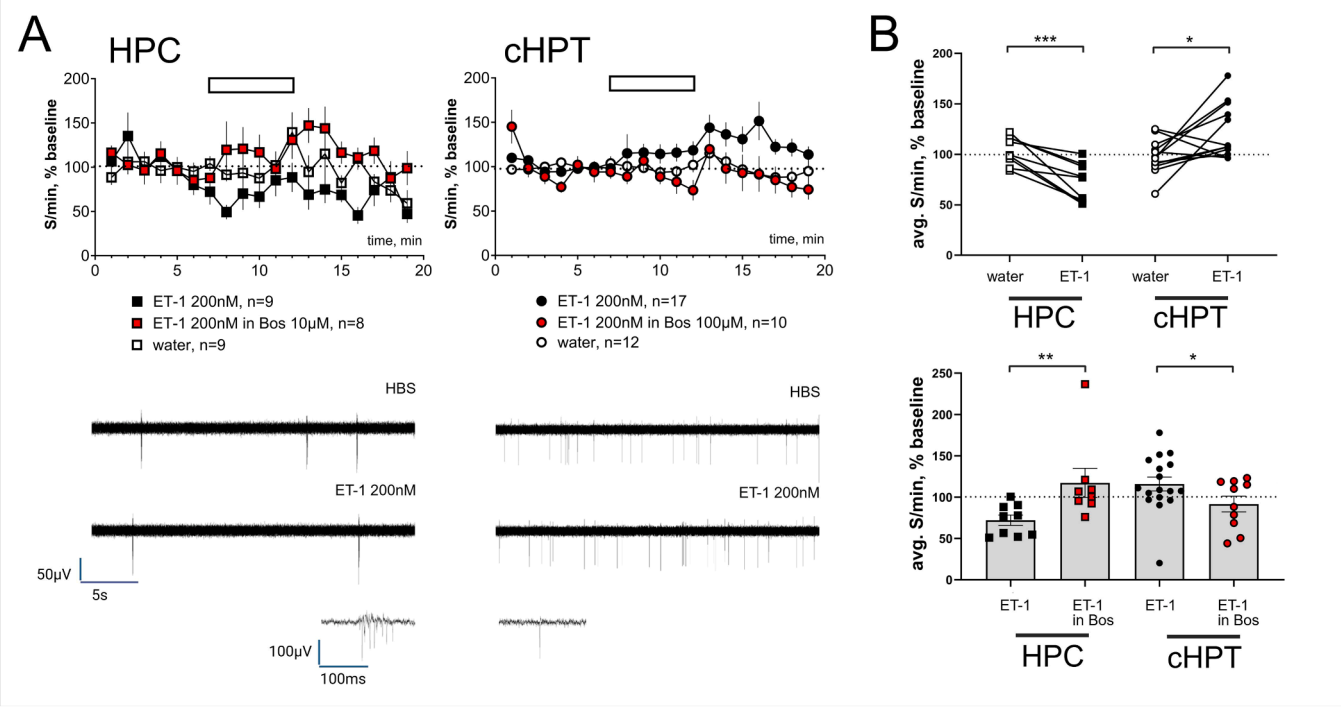

Fig. 1. ET-1 modulates neuronal firing rate in HPC and cHPT cultures through ET-receptors **A**. Time-course diagrams of total number of Spikes/min in HPC (left) and cHPT (right) shown as percent of 7 min baseline. Application periods of ET-1 200 nM and water are indicated by an open bar above individual datapoints. Representative examples of MEA recordings are shown below plots. Voltage traces show firing patterns during control phase (HBS) and ET-1 200 nM application period in HPC and cHPT, at the bottom examples of action potentials in HPC (burst-like firing) and cHPT (single spike firing) are shown enlarged **B.** Paired *t*-test compares the 5-minute averages during application period of ET-1 to vehicle control (upper plot) and unpaired *t*-test and Mann-Whitney *U* Test compare average ET-1 control responses during application period with the response in the presence of bosentan (lower plot). n.s.: not significant; *:$p < 0.05$; **:$p < 0.01$,***:$p < 0.001$.

excitation in cHPT reached in the second minute of the washout period to 263.3 ± 22.4% of baseline. Similar to the averaged S/min across all MEA electrodes (Fig. 1A), maximum inhibition in HPC was reached during the first minute of ET-1 application to 45.4 ± 2.7% of baseline. For both cHPT and HPC, inhibited channels do not return to baseline activity with a stronger rundown observed in HPC. In recordings of HPC (n = 9, N = 5), 64 channels (95.5% of all responding channels) were inhibited and 3 excited. In cHPT recordings (n = 17, N = 12), a total of 107 channels were inhibited (33.1% of all responding channels) and 216 channels were excited. Fisher's exact probability test revealed a significant difference in effect probability between HPC and cHPT ($p < 0.0001$).

Taken together, these results show that ET-1 induces region-dependent responses with predominant inhibition in the hippocampus and excitation in the caudal hypothalamus, respectively.

3.3. ET-1 increases bursting and network synchrony of cHPT cultures and decreases bursting of HPC cultures via ET-receptors

Synchrony of neuronal discharge (Cohen's kappa or "kappa") and bursts per minute (B/min), as illustrated by the time course diagrams (Fig. 3A) and averages of the 5-minute application period (Fig. 3B), were differentially affected by ET-1 in HPC and cHPT.

In HPC, kappa was not significantly altered by ET-1 200 nM (n = 9, N = 5) in comparison to water control during the 5-minute application period (Fig. 3B, top, unpaired *t*-test, $t(16) = 0.49$, $p = 0.62$) and remained at 103.1 ± 3.3% of baseline. In contrast, ET-1 application led to a significant decrease in B/min to 69.1 ± 8.2% of baseline (Fig. 3B, bottom, unpaired *t*-test, $t(16) = 3.67$, $p = 0.002$) which was significantly attenuated by bosentan 10 µM (n = 8, N = 7, Fig. 3B, bottom, unpaired *t*-test, $t(15) = 2.76$, $p = 0.01$). HPC was characterized by highly synchronized baseline activity (Fig. 3C, D, left) that was visibly not altered by ET-1 application (Fig. 3C, left) with an average raw kappa value of 0.74 ± 0.04 during the baseline and 0.77 ± 0.04 during the washout period.

A different response was observed in cHPT, where kappa relative to baseline was significantly increased by ET-1 200 nM (n = 15, N = 10) during the average 5-minute application period compared to water control (Fig. 3B, top, MWT, U (N1 = 10, N2 = 15) = 30, $p = 0.01$) on average to 165.5 ± 17.8% of baseline. Similarly, the number of bursts per minute (B/min) was significantly increased in cHPT (Fig. 3B, bottom, unpaired *t*-test, $t(23) = 2.5$, $p = 0.02$) on average to 150.6 ± 16.8% of baseline. The visibly asynchronous spike-like firing pattern under baseline conditions (Fig. 3C, D, right) shifted toward higher synchrony with a notable increase in bursting during ET-1 application (Fig. 3C, right). The average raw kappa value increased from 0.1 ± 0.01 during the baseline period to 0.15 ± 0.02 during the application period. In the presence of bosentan (n = 10, N = 6), effects of ET-1 on kappa values in cHPT cultures were negligible, represented 110.3 ± 9% of baseline and significantly differed from recordings without antagonist (Fig. 3B, top, MWT, U (N1 = 10, N2 = 15) = 33, $p = 0.02$). The effect of ET-1 on B/min in the presence of bosentan represented 103.6 ± 11.5% of baseline and differed significantly from ET-1 application (Fig. 3B, bottom, unpaired *t*-test, $t(23) = 2.07$, $p = 0.0497$).

Both parameters (kappa and B/min) did not differ from the water control in the presence of bosentan (Fig. 3B, kappa: HPC: MWT, U (N1 = 8, N2 = 9) = 34, $p = 0.89$; cHPT: unpaired *t*-test, $t(18) = 0.35$, $p = 0.73$; B/min: HPC: unpaired *t*-test, t(15) = 1.13, $p = 0.27$; cHPT: unpaired *t*-test, $t(18) = 0.5$, $p = 0.62$).

In cHPT, the average kappa during the 5-minute application as % of the baseline positively correlated with the average bursts as % of baseline (Fig. 3E, Pearson correlation coefficient $r = 0.58$, $p = 0.023$). These results show that ET-1 enhanced the neuronal network synchrony likely through an increase in burst-like activity, whilst no synchronizing effect

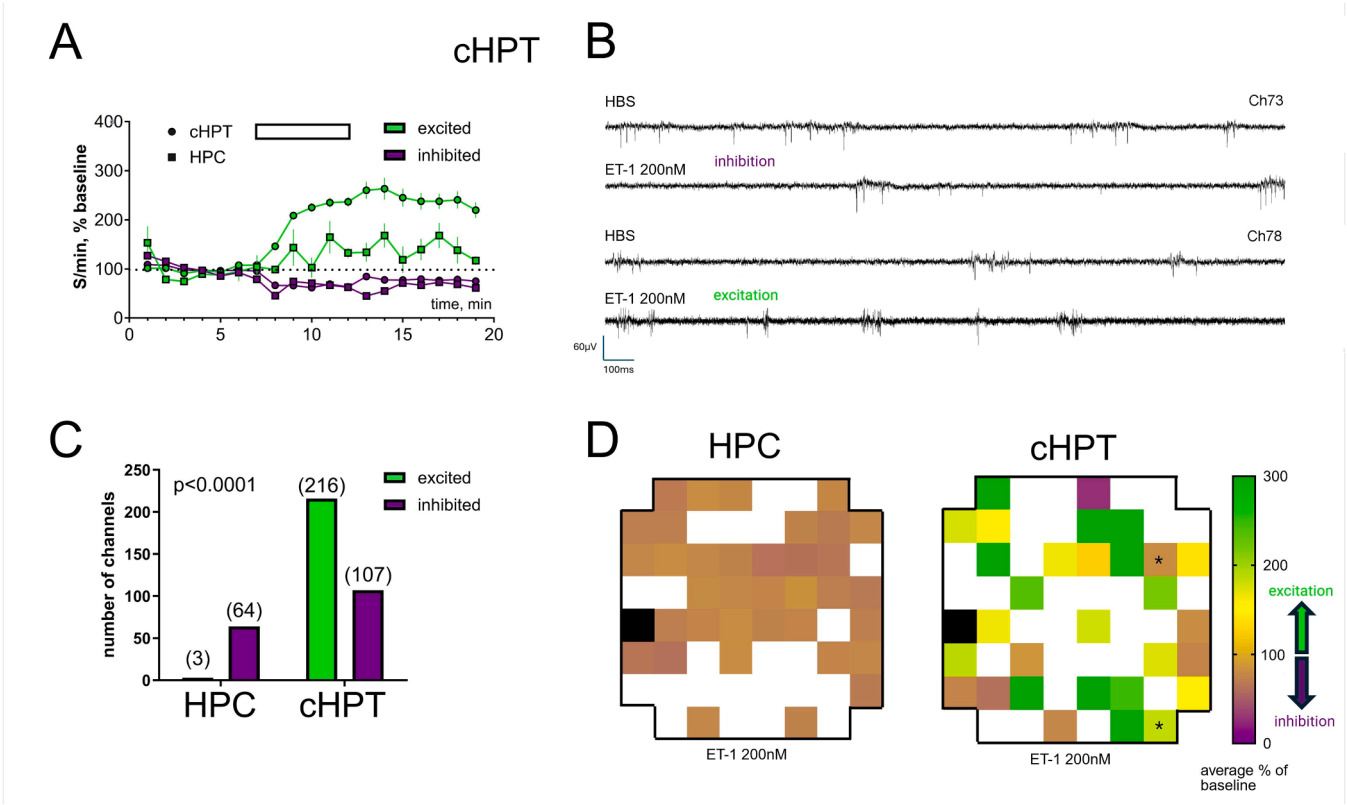

Fig. 2. Single MEA channel analysis reveals heterogenous effects of ET-1 application on FFR in HPC and cHPT. **A.** Time-course diagrams of average Spikes/min in detected excited and inhibited channels of HPC and cHPT from all recordings shown as percent of 7 min baseline with a 5-minute application period of ET-1 200 nM indicated by an open bar above individual datapoints **B.** Exemplary effect of ET-1 application compared to control (HBS) in channels that were detected as excited (Channel 78) or inhibited (Channel 73) from representative MEA recording of cHPT **C.** Fisher's exact probability test (FEPT) for difference in effect probability (excited or inhibited channels) between HPC and cHPT. **D.** Heatmaps illustrate the spatial appearance of ET-1-mediated excitation or inhibition in neuronal networks in one representative recording from each culture type. Schematic drawings of a 60-electrode grid of MEA-60 (Cat. No. 890953) where each square box is one field recorded by one electrode. Relative firing frequency of each electrode (Spikes per min in percent of baseline, averaged for the whole application period of ET-1) is encoded by color, with the maximal increase in frequency (excitation) in green and the maximal decrease (inhibition) in purple. Inactive and unchanged channels are shown in white, ground electrode (Channel 15) in black. Two asterisks (*) on MEA grid covered by cHPT show position of Channel 73 (asterisk in upper right corner, in brown field, indicates inhibition) and Channel 78 (asterisk in lower right corner in green field indicates excitation by ET-1); recordings from these 2 channels in the same experiment are shown in **B**.

was seen for neuronal network activity of the hippocampus, which was accompanied by a decline in bursting. Increase in kappa and B/min of cHPT and decrease in B/min in HPC were blocked by dual ET-receptor antagonist bosentan.

3.4. ET_A and ET_B expression ratio differs between HPC and cHPT

HPC expressed 1.6 times more ET_A than cHPT (Fig. 4A, paired *t*-test, t (18)= 7.2, $p < 0.0001$). Expression of ET_A differed neither between HPC of males (123 ± 18%, n = 8) and females (101 ± 8%, n = 11, $p = 0.22$, t (17) = 1.3) nor between cHPT of males (80 ± 10%, n = 8) and females (62 ± 7%, n = 11, $p = 0.16$, $t(17) = 1.5$).

cHPT was characterized by 1.8 times higher expression of ET_B than HPC (Fig. 4B), which was significant according to the paired *t*-test (t (18) = 6.7, $p < 0.0001$). There were no sex-specific differences in ET_B expression in HPC (121 ± 15%, n = 11 in females and 144 ± 20%, n = 8 in males, $t(17) = 1.0$, $p = 0.35$) or in cHPT (202 ± 29%, n = 11 in females and 290 ± 39%, n = 8 in males, MWT, U (N1 = 8, N2 = 11) = 23, $p = 0.09$).

Taken together, HPC expressed proportionally more mRNA encoding for the ET_A receptor whilst cHPT expressed proportionally more ET_B receptor transcripts.

3.5. ET-1 induces a delayed bosentan-sensitive inhibition of DGgc and excitation of HN

All neurons that were recorded in brain slices with the patch-clamp technique were selected in defined anatomical regions and possessed typical firing patterns of electrical activity. HN were recorded in the ventrolateral TMN. They showed spontaneous firing in a range between 0.32 and 8.4 Hz (3.2 ± 0.47 Hz on average) and were pharmacologically identified by application of H3-receptor agonist (R)(−)-α-Methylhistamine (RAMH, 2 µM), which reduced firing frequency to 53.7 ± 4.9% of baseline (5th application minute, 23 neurons, see supplementary Fig. 1). H3-receptor antagonist clobenpropit (20 µM), which was applied in some cells after RAMH withdrawal, increased firing of HN to 167 ± 9.9% of baseline (n = 9), supporting an expression of the H3-receptor, a typical feature of HN (see [34]). DGgc were recorded in the granule cell layer of the dentate gyrus as described in [26].

Compared to the baseline period, ET-1 did not induce a significant change in firing frequency during the 7 min of ET-1 application period either in DGgc (repeated-measures one-way ANOVA, $F(2,24) = 5.592$, $p = 0.01$; Dunnett's multiple comparisons test, $p = 0.67$) or in HN (Friedman Test, χ^2 (2) = 12.78, $p = 0.0017$, Dunn's multiple comparisons test, $p = 0.08$). A significant difference in frequency change during the ET-1 application period in the presence and absence of bosentan was detected in HN (Fig. 5B, right, paired *t*-test, $t(22) = 4.94$, $p < 0.0001$)

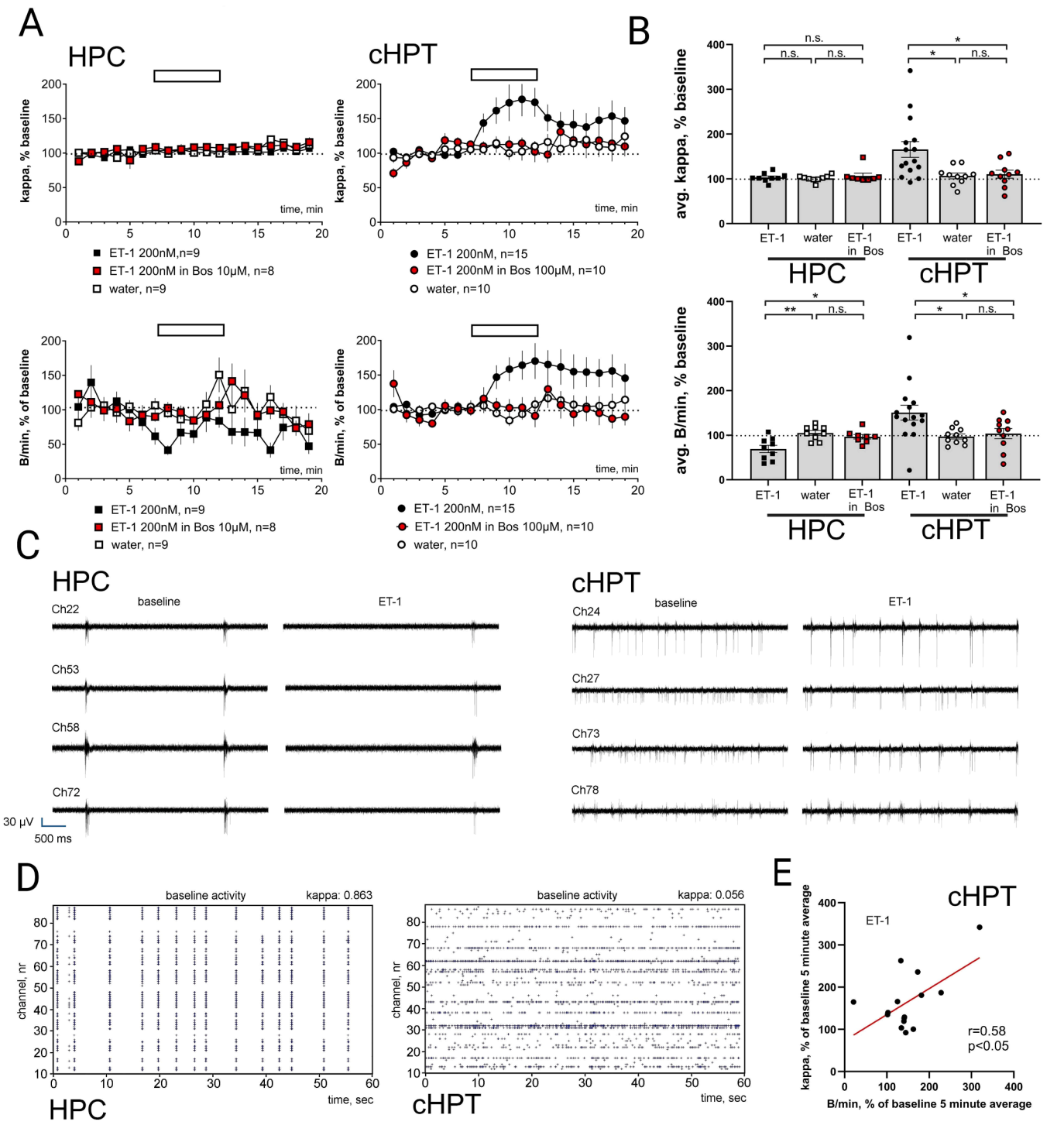

Fig. 3. ET-1 induces an increase in bursting and network synchrony in cHPT and decrease in bursting in HPC cultures **A**. Time-course diagrams of kappa (top) and bursts/min (bottom) in HPC (left) and cHPT (right) as % of 7-minute baseline period with 5-minute application of water, ET-1 or ET-1 in bosentan (Bos), indicated by an open bar above individual datapoints **B.** Comparison of 5-minute average of kappa (top) and bursts/min (bottom) as % of baseline in ET-1, vehicle control (water) and ET-1 in bosentan **C.** Representative traces of extracellular action potentials from selected MEA channels in HPC (left) and cHPT (right) each captured during the same timepoint during baseline (left) and ET-1 application (right) **D.** Spike-raster plots of representative MEA-recordings of HPC and cHPT during baseline period, x-axis represents recording time, rows on y-axis represent individual MEA-channels, dots show a detected spike. Cohen's kappa values are shown above the plots **E.** Correlation analysis between average kappa and B/min as % of baseline during 5-minute ET-1 200 nM application. n.s.: not significant; *:$p < 0.05$; **:$p < 0.01$.

but not in DGgc (Fig. 5B, left, paired *t*-test, $t(12) = 1.484, p = 0.16$). This seemingly paradoxical observation (no effect of ET-1 but a significant difference between ET-1 and ET-1 in bosentan in HN) can be explained by an endogenous tonic activation of endothelin receptors in slices and their block in the presence of bosentan. Firing frequency changes in HN (Fig. 5A, right) amounted to 0.1 ± 0.09 Hz during the ET-1 application alone ($n = 23$, $N = 19$) and to -0.21 ± 0.1 Hz during application of ET-1 with bosentan. Control ET-1 application decreased firing frequency of DGgc (Fig. 5A, left, $n = 13$, $N = 11$) to -0.45 ± 0.42 Hz; during co-application of peptide with antagonist, the frequency changes

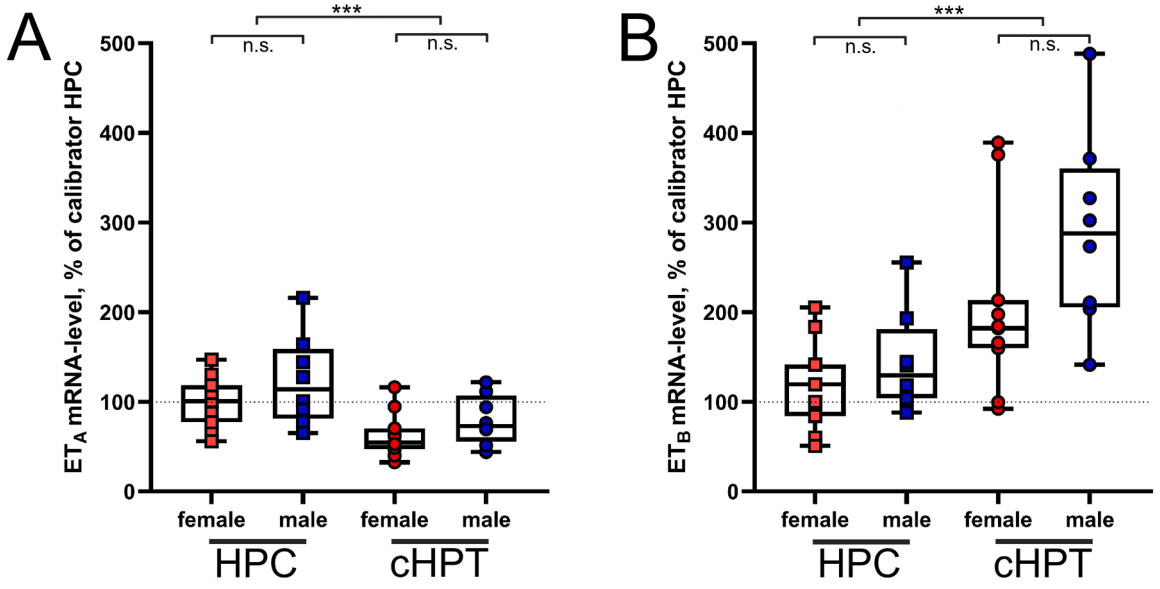

Fig. 4. Ratios of ET_A and ET_B mRNA-expression differ between HPC and cHPT **A.** ET_A expression in HPC and cHPT of female (red) and male (blue) mice as % of female calibrator HPC. No significant sex-specific differences in ET_A expression detected within either region (paired *t*-test). Paired *t*-test detects a significantly higher ET_A expression in HPC compared to cHPT by 1.6 fold. **B.** ET_B expression in HPC and cHPT of female (red) and male (blue) mice as % of female calibrator HPC. No significant sex-specific differences in ET_B expression detected within either region (MWT). Paired *t*-test detects a significantly higher ET_A expression in cHPT compared to HPC by 1.8 fold. n.s.: not significant; ***:$p < 0.001$.

amounted to 0.44 ± 0.31 Hz.

In DGgc, a significant difference between the baseline and 12 min washout period was detected after ET-1 application (repeated-measures one-way ANOVA (see above), Dunnett's multiple comparisons test during the washout phase, $p = 0.007$) with a decrease in firing frequency (−1.92 ± 0.7 Hz) which was significantly attenuated by bosentan (Fig. 5B, left,+1.11 ± 0.71 Hz, paired *t*-test, $t\ (12) = 2.239$, $p = 0.04$). HN showed a significant increase in firing frequency (Friedman Test as above, $p = 0.0017$, Dunn's multiple comparisons test with baseline, $p = 0.001$) during the 12 min of ET-1 withdrawal (+0.39 ± 0.15 Hz) which was significantly impaired by the antagonist (Fig. 5B, right, frequency reduced to −0.11 ± 0.16 Hz, paired *t*-test for control ET-1 response vs. ET-1 and bosentan in the same neuron, $t(22) = 3.618$, $p = 0.002$).

A significant difference in the occurrence of excitation during and after ET-1 application alone or in the presence of antagonist (number of cells showing excitation, inhibition or no change are analyzed under 2 different conditions with Chi-square test) was detected in HN ($p = 0.007$ and $p = 0.012$ for application and washout periods, respectively). In contrast, Chi-square test did not show a significant difference in the occurrence of inhibition in DGgc between control ET-1 response and response in bosentan. No differences in ET-1 effects were detected between male and female mice (no significant interaction between sex and time) of DGgc (repeated-measures two-way ANOVA, $F(2,22) = 0.34$, $p = 0.71$) and HN (repeated-measures two-way ANOVA, $F(2,42) = 0.17$, $p = 0.84$). This is in line with our observation that ET-receptor expression of HPC and cHPT did not significantly differ between sexes (see 3.4). In summary, the responses to ET-1 application in DGgc and HN displayed region-specific temporal dynamics, with a delayed bosentan-sensitive excitation in HN and inhibition in DGgc during the washout period.

3.6. Single-cell RT-PCR detects expression of ET-receptors in HN and DGgc

Using single-cell RT-PCR, we identified DGgc (Fig. 6A, top) and HN (Fig. 6A, bottom) with the markers PDZd2 and HDC. Among the 26 PDZd2-positive DGgc, 13 (50%) were expressing ET_B receptor, whereas ET_A was detected in no DGgc (supplementary Fig. 2 A). Among all cells harvested from the DG, 22 were PDZd2-negative and excluded from further analysis. Of the 22 identified HN, 15 were expressing ET_B receptor (68%). Among the ET_B-positive HN, 4 were coexpressing ET_A receptor (18% of total HDC-positive cells, supplementary Fig. 2B). Four harvested red HN cells from Tmt-HDC mice were PCR-negative and excluded from receptor analysis.

4. Discussion

The major finding of the present study is that endothelin-1 induces a delayed increase in neuronal firing rate of identified histaminergic neurons (HN) in slice recordings and an increase in firing frequency, synchrony of discharge and bursting of hypothalamic neurons cultured on MEAs. Dual-endothelin receptor antagonist bosentan impaired the delayed ET-1-induced increase in firing frequency of HN in brain slices. In line with previous studies [3], the hippocampal network was predominantly inhibited by ET-1. Our patch-clamp recordings from DGgc in brain slices were in line with our observation on cultures (ET-1- induced delayed inhibition of firing, which was abolished by bosentan). Half of the identified DGgc and 68% of HN expressed ET_B receptor (single-cell RT-PCR); 18% of HN co-expressed ET_A and ET_B receptors, whereas none of DGgc expressed ET_A receptor.

This result is surprising, as HPC tissue expressed higher levels of ET_A but lower levels of ET_B compared to cHPT (qPCR). Previous studies have shown that ET_B is the dominant receptor type in the brain [35]. Different cell types may express endothelin peptides and receptors e.g. endothelial cells, glial cells, as well as vascular and glial precursors, as shown in a study on the single-cell transcriptome of the murine caudal hypothalamus [36] as well as the human proteome atlas [37].

Can the expression of ET_A receptor in HN explain the excitatory response to ET-1? ET-1-mediated excitation is described to occur primarily via ET_A receptor [21] and inhibition via ET_B receptor [4]. Therefore we hypothesized that a subset of HN expresses excitatory ET_A, which may make them directly responsive to ET-1 and may influence cellular circuits relevant to the regulation of arousal. In the hippocampus, ET_A receptor is expressed primarily in the mossy fiber pathway, whereas ET_B receptor can be found primarily in pyramidal cells, granule

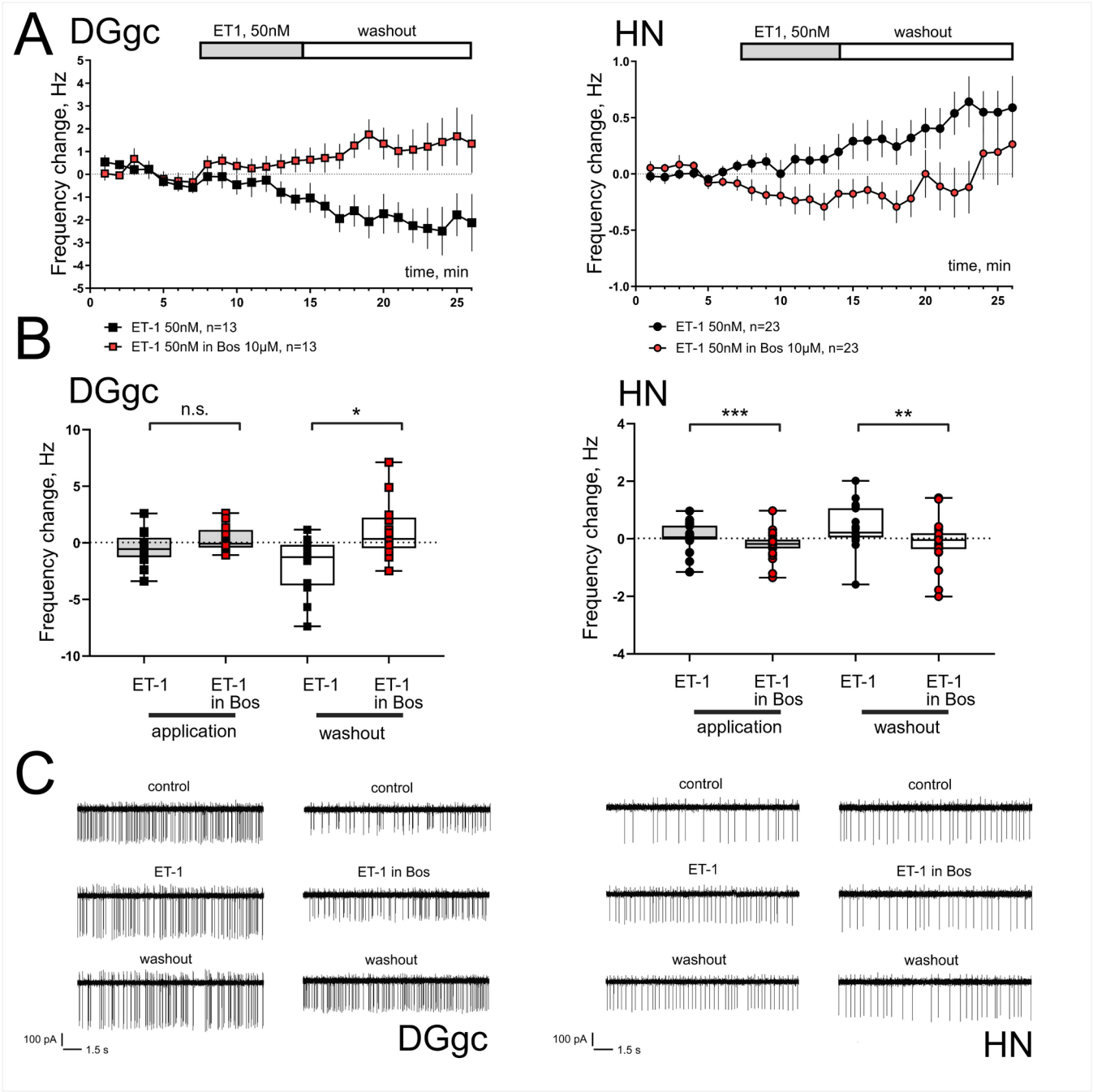

Fig. 5. ET-1 induces a bosentan-sensitive delayed inhibition of DGgc and excitation of HN **A**. Time course diagrams of changes in firing frequency (Hz) of DGgc (left) and HN (right) showing 7-minute application of ET-1 50 nM in the absence or presence of bosentan 10 µM, followed by washout **B.** Paired *t*-test shows a significant difference between ET-1 and ET-1 in bosentan in the washout period in DGgc and during both: application and washout periods of HN. Boxes represent the interquartile range, whiskers show minimum and maximum values, individual data points represent averages (1 per cell) of indicated time periods **C.** Representative recordings of DGgc (left) and HN (right) showing control period, ET-1 application with and without bosentan and washout period. n.s.: not significant; *:$p < 0.05$; **: $p < 0.01$; ***:$p < 0.001$.

cells and glial cells [38]. Chen et al. have shown a decrease in firing of hippocampal pyramidal neurons in response to ET-1 application producing anxiolytic effects [3]. The opposite regulation that was observed in hypothalamic and hippocampal neurons likely reflects differences in receptor expression patterns indicated by our qPCR and scRT-PCR data. In contrast to DGgc, we were able to detect expression of ET_A receptor in identified HN. In addition, the hippocampal and hypothalamic networks differed substantially in their baseline firing patterns (Fig. 3C, D) which could further induce region-specific responses to ET-1.

To exclude polysynaptic effects, we performed our patch-clamp experiments in calcium-free ACSF, which prevents the release of neurotransmitters. In some of our pilot experiments, we applied ET-1 in the presence of gabazine ($GABA_A$-receptor antagonist). This treatment did not affect the responsiveness to peptide. Lack of significance in the occurrence of ET-1-induced inhibition in control ACSF versus ACSF with bosentan can be explained by a low probability of response (6 DGgc out of 13), which can be underlined by a low expression rate of ET_B receptor (50%). Low response probability was also detected in HN (significant excitation in 8 cells and in 11 cells out of 23 investigated neurons during application and washout phase, respectively). This prevented us from

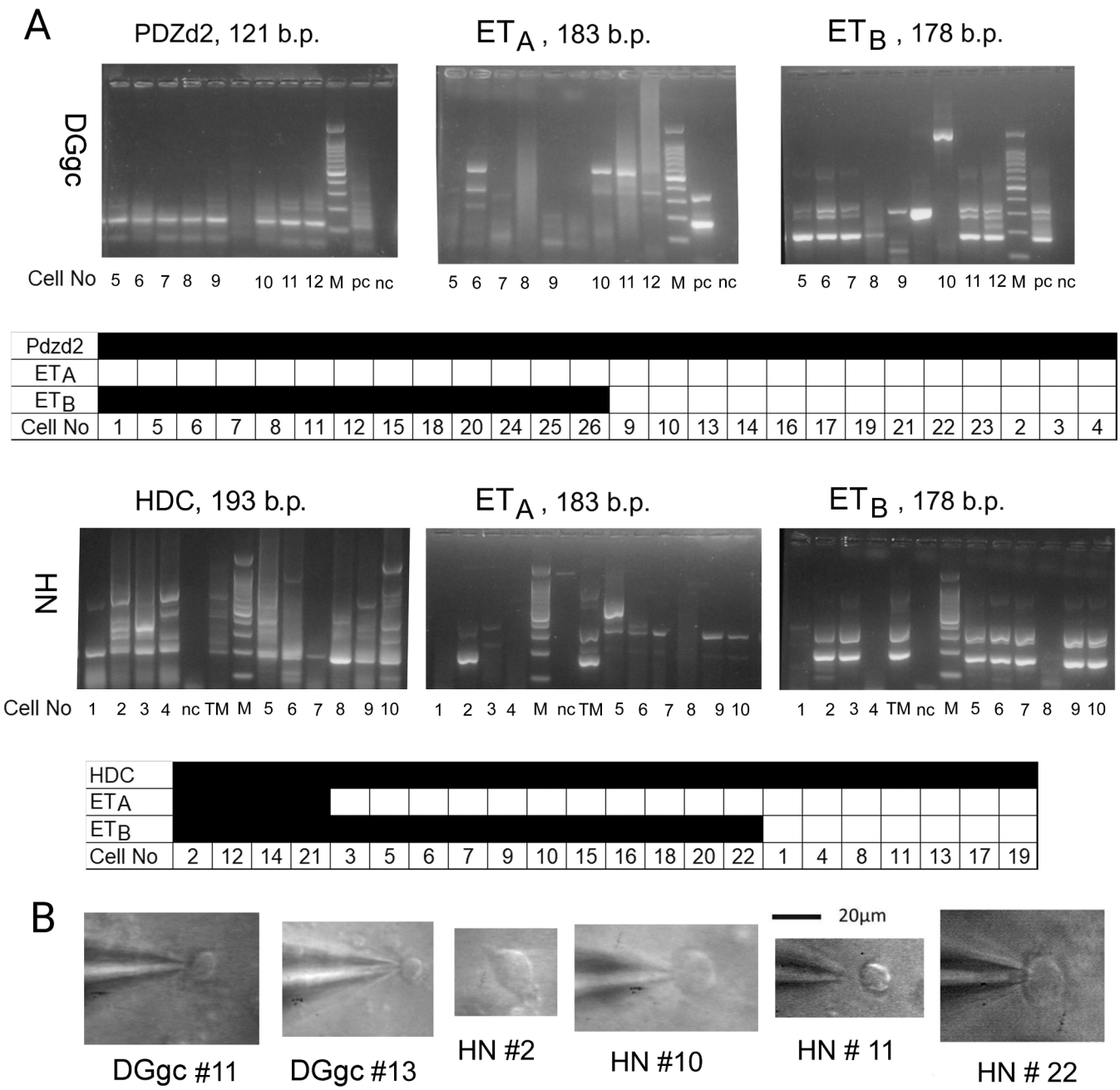

Fig. 6. Difference in ET_A and ET_B expression detected between DGgc and HN using single-cell RT-PCR **A.** Identifcation of DGgc by detection of PDZd2 and HN by Histidine Decarboxylase (HDC). Representative photographs of gels illustrating analysis of ET_A and ET_B expression in individual neurons, M: DNA size marker 100 b. p. ladder (Promega, Cat. No G2101), the 500 b.p. band is present at triple intensity of the other fragments; nc: negative control, pc: positive control (HPC or TM: region around ventrolateral tuberomammillary nucleus). Below the gels are floating bar graphs illustrating the co-expression pattern of ET_A and ET_B in DGgc (top) and HN (bottom) **B.** representative photographs of harvested cells.

performing an application of receptor type-specific antagonists as we followed 3 R (replace, reduce, refine) principles for animal experiments. As bosentan reduced the ET-1-induced increase in synchronous neuronal discharge of cultured cHPT neurons, increase in bursting and increase in firing rate, one can suggest an involvement of ET-receptors in the regulation of firing pattern and synchrony of discharge of hypothalamic neurons. High neuron-to-neuron heterogeneity in responsiveness to ET-1 prompted us to design a program for automatic sorting of active MEA channels to separate inhibition from excitation. Separate analysis of excited and inhibited neurons provided the first proof of concept that such high-throughput analysis can be performed. Further studies with conditional knockout mice with ET_A-deficient HN may be more conclusive in answering the question whether ET-1 induced excitation depends on ET_A receptor.

One potential mechanism through which ET-1 may modulate neuronal activity would be the direct modulation of ion channels via ET-receptors. In cultured cerebellar granule cells, ET-1 inhibits voltage sensitive L-Type Ca^{2+} channels through ET_A receptor [39]. In dorsal root ganglion, ET-1 excites nociceptors through signal cascades triggered by ET_A. As a result, inhibition of delayed rectifier potassium channels [22], enhancement of currents through TRPV1 [40] and acid-sensing ion channels (ASICs) [41] are occurring. HN also express ASICs [42,43] and TRPV1 [31,42], which function as excitatory receptors on HN. The role of these channels in ET-1-mediated excitation of HN remains to be

elucidated.

It should be noted that ET-1 may influence neuronal activity through the modulation of glial cells, which express ET-receptors. Endothelin-1 increases 2-arachidonoyl glycerol (2-AG) production in astrocytes, an agonist for CB1 and CB2 receptors [44]. Activation of the CB1 and CB2 receptors is known to increase histamine release in the TMN [45] and to increase the firing rate of HN recorded in mouse brain slices [31]. Furthermore, ET-1 reduces glutamate uptake in primary cultures of rat astrocytes [46]. Glutamatergic neurotransmission excites HN and triggers histamine release [42,47]. Also, ET-1 evokes a rise in calcium level in astrocytes of the supraoptic nucleus through ET_B receptors [19].

How can ET-1 change the firing pattern of cultured hypothalamic neurons from regular firing to synchronous bursting? It is known that the switch of neuronal firing pattern towards bursting activity depends on ion channel modulation. Small-conductance calcium-activated potassium channel (SK-channel) inhibition is required for burst initiation and modulation in spinal motoneurons [48]. Large-conductance calcium-activated potassium channel (BK-channel) inhibition in cerebellar Purkinje neurons induces burst firing [49]. Interestingly, in striatal astrocytes ET-1 is capable to modulate SK- and BK- channels [50]. Burst generation in the ventromedial hypothalamus depends on sodium channels and coupling via gap junctions [51]. ET-1 uncouples gap junctions in cultured astrocytes [52], but role of this peptide for the modulation of neuronal gap junctions is still unclear. Thus, mechanisms explaining the induction of bursting and increase in synchrony of neuronal firing in cHPT cultures, induced by ET-1 via ET-receptors, await further elucidation. The lack of ET-1 effects on network synchrony of hippocampal cultures could be explained by the highly synchronized burst-like activity under baseline conditions (see Fig. 3C, D, left).

How can long-term inhibition of activity in HPC cultures by ET-1 be explained? Control water application did not induce a similar "rundown"-like effect. We hypothesize that gliotransmitters may be involved in this modulation, as glia expresses ET-receptors [36]. Astrocytic release of ATP likely increases adenosine levels, which may slowly accumulate and inhibit hippocampal neurons, but not HN, through the adenosine 1 receptor (A1R) [26].

Strength of the present study lays in combination of two different cellular approaches with both showing modulatory activity of ET-1. While neurons identified within the native local circuitry were recorded one by one with patch-clamp technique in slices, hippocampal or hypothalamic networks were studied in primary dissociated cultures grown on MEAs, where multi-channel recordings revealed that excitation or inhibition by ET-1 appear at the same time on different spatially separated electrodes. Thus, it is unlikely that bidirectional ET-1 modulation, also observed in slice recordings, depends on circadian factor. It can be proposed that ET-receptors, signal transduction mechanisms and/or local microenvironment determine the direction of response.

Several limitations of the present study need to be considered. We used in our experiments ET-1 in concentrations 50 and 200 nM and it remains possible that some effects were not detected due to the peptide concentration used. Physiologically, ET-1 is expressed in the brain in the picomolar range [53]. Thus, one needs to be careful to extrapolate our findings to brain physiology. Most electrophysiological studies use similar ET-1 concentrations as in our study [5,22,39,41,50,54]. Applying such high concentrations of peptide increases the probability of response detection due to the low receptor expression in neurons and glial cells. In our pilot experiments we were not able to obtain a reliable response with picomolar concentrations either in MEA or in patch-clamp recordings. Another important limitation is that MEA recordings and patch-clamp recordings represent substantially different model systems. Primary dissociated cultures measured with MEAs lack long-range connections and pathways and display differences in network organization. Cultured neurons as used in our study originate from postnatal tissue. Thus, tissue maturation occurs *in vitro,* which may influence receptor expression profiles, with differential expression profiles previously described depending on the age of primary cultures [55]. One advantage of the MEA method is that responses of neurons can be studied in a system essentially devoid of vasculature. Primary neuronal cultures are essentially free of endothelial cells [56]. However, the occasional survival of vascular cells in our cultures cannot be excluded. Using calcium-free ACSF in patch-clamp experiments, we tried to avoid artifacts caused by tissue movements and vasoconstriction described in a previous study [20].

In contrast to MEA experiments, brain slices for patch-clamp recordings were prepared in our study from adult animals and preserve the local neuronal circuitry and long-range connections. However, slices are exposed to conditions like hypoxia that may influence ET-1 and ET-receptor expression and function [53,57,58].

Therefore, the findings of the present study should be validated in future studies with the recordings from HN *in vivo* in combination with behavior (sleep-wake EEG recordings).

Histaminergic neurotransmission is modulated by several neuropeptides, including orexin, TRH and substance P [12–14]. Orexinergic modulation is regarded as one of the major excitatory signals promoting wakefulness through a robust activation of HN [12]. Compared with these established modulators of HN, our observed ET-1 effects on the firing rate of HN appear weaker and temporally dissociated. The increase in synchrony and bursting in cHPT cultures developed rapidly during the application of the peptide, whereas the increase in firing frequency in identified HN in patch-clamp slice recordings developed delayed during the washout period. This indicates that ET-1 initially modulates network-level synchrony whilst changes in HN excitability may involve slower mechanisms. Therefore, it is likely that ET-1 may function as a weak modulator that influences hypothalamic excitability under specific physiological or pathological conditions.

ET-1 is involved in circuits processing anxiety and stress [3,4]. The inhibition of hippocampal CA1 pyramidal neurons by ET-1 correlates with anxiolytic effects of the peptide in mice and down-regulation of ET-1 expression enhances anxiety [3]. Furthermore, ET-1 levels are known to be elevated in response to hypoxia or ischemia *in vitro* [57,58] and *in vivo* [53]. There have been studies indicating that hypothalamic ET-1 levels are elevated in response to chronic and acute stress states such as inflammation and fever [59] and may modulate stress responses and autonomic outputs synergistically with catecholamines, with immunohistochemistry showing a colocalization of ET-1 with Tyrosine-Hydroxylase (TH) in the hypothalamus [60]. In the posterior hypothalamus, ET-1 increases TH activity through a G-protein-coupled receptor [61]. ET-1 increases *in vitro* norepinephrine (NE) release in the posterior hypothalamus [62]. Although there is no direct evidence that NE changes the firing properties of HN directly, it indirectly excites HN by inhibiting presynaptic GABAergic inputs through α2-adrenoreceptors [63]. Taken together, ET-1 may be released in states of stress and hypoxia and contribute to the release of wake-promoting histamine, potentially activating neuronal circuits of arousal regulation by directly or indirectly exciting HN.

We show for the first time an interaction between the brain endothelin system and firing properties of central histaminergic neurons *in vitro*. ET-1 increases the firing frequency and network synchrony in caudal hypothalamic neurons through ET-receptors, which may influence histaminergic neurotransmission and link certain ET-1-induced vascular and stress signals to arousal states on a cellular level. Further studies should explore mechanisms of ET-1 action and delineate signaling pathways that mediate the increase in network synchrony and bursting, as well as the delayed HN excitation. Moreover, behavioral responses to endothelin receptor activation should be studied *in vivo* across the sleep-wake cycle.

Funding

This research did not receive any specific grant from funding agencies in the public, commercial, or not-for-profit sectors. Open

Access funding enabled and organized by Projekt DEAL.

CRediT authorship contribution statement

Lea Wegmann: Writing – review & editing, Writing – original draft, Visualization, Methodology, Investigation, Formal analysis, Data curation, Conceptualization. **Morris Haid:** Writing – review & editing, Software, Formal analysis. **Dennis Thomassen:** Writing – review & editing, Methodology, Conceptualization. **Olga A. Sergeeva:** Writing – review & editing, Writing – original draft, Visualization, Supervision, Resources, Project administration, Methodology, Investigation, Formal analysis, Data curation, Conceptualization.

Declaration of Competing Interest

The authors declare the following financial interests/personal relationships which may be considered as potential competing interests: Given her role as associate editor, Olga A. Sergeeva had no involvement in the peer-review of this article and has no access to information regarding its peer-review. Full responsibility for the editorial process for this article was delegated to another journal editor. Other authors declare that they have no known competing financial interests or personal relationships that could have appeared to influence the work reported in this paper

Acknowledgements

We are grateful to Thomas Becher and Stephan Schätz for excellent technical support with computers and experimental devices and Prof. Dr. med. Helmut L. Haas for valuable comments and suggestions on manuscript.

Appendix A. Supporting information

Supplementary data associated with this article can be found in the online version at doi:10.1016/j.peptides.2026.171495.

Data availability

Data will be made available on request.

References

[1] M. Yanagisawa, H. Kurihara, S. Kimura, Y. Tomobe, M. Kobayashi, Y. Mitsui, Y. Yazaki, K. Goto, T. Masaki, A novel potent vasoconstrictor peptide produced by vascular endothelial cells', Nature 332 (6163) (1988) 411–415.
[2] M. Barton, M. Yanagisawa, Endothelin: 30 years from discovery to therapy, Hypertension 74 (6) (2019) 1232–1265.
[3] M. Chen, S. Shu, H.H. Yan, L. Pei, Z.F. Wang, Q. Wan, L.L. Bi, Hippocampal Endothelin-1 decreases excitability of pyramidal neurons and produces anxiolytic effects, Neuropharmacology 118 (2017) 242–250.
[4] M. Chen, H.H. Yan, S. Shu, L. Pei, L.K. Zang, Y. Fu, Z.F. Wang, Q. Wan, L.L. Bi, Amygdalar Endothelin-1 regulates pyramidal neuron excitability and affects anxiety, Sci. Rep. 7 (1) (2017) 2316.
[5] N.K. Mule, J.N. Singh, K.U. Shah, A. Gulati, S.S. Sharma, Endothelin-1 decreases excitability of the dorsal root ganglion neurons via et(b) receptor, Mol. Neurobiol. 55 (5) (2018) 4297–4310.
[6] A. Gulati, M.G. Hornick, S. Briyal, M.S. Lavhale, A novel neuroregenerative approach using ET(B) receptor agonist, IRL-1620, to treat CNS disorders, Physiol. Res 67 (1) (2018) S95–S113.
[7] L.G. Douma, D. Barral, M.L. Gumz, Interplay of the circadian clock and endothelin system, Physiol. (Bethesda) 36 (1) (2021) 35–43.
[8] A. Pizarro, K. Hayer, N.F. Lahens, J.B. Hogenesch, CircaDB: a database of mammalian circadian gene expression profiles, Nucleic Acids Res 41 (2013) D1009–1013 (Database issue).
[9] Y. Nakahata, M. Akashi, D. Trcka, A. Yasuda, T. Takumi, The in vitro real-time oscillation monitoring system identifies potential entrainment factors for circadian clocks, BMC Mol. Biol. 7 (2006) 5.
[10] N. Takashima, A. Fujioka, N. Hayasaka, A. Matsuo, J. Takasaki, Y. Shigeyoshi, Gq/11-induced intracellular calcium mobilization mediates Per2 acute induction in Rat-1 fibroblasts, Genes Cells 11 (9) (2006) 1039–1049.
[11] H.L. Haas, O.A. Sergeeva, O. Selbach, Histamine in the nervous system, Physiol. Rev. 88 (3) (2008) 1183–1241.
[12] K.S. Eriksson, O. Sergeeva, R.E. Brown, H.L. Haas, Orexin/hypocretin excites the histaminergic neurons of the tuberomammillary nucleus, J. Neurosci. 21 (23) (2001) 9273–9279.
[13] R. Parmentier, S. Kolbaev, B.P. Klyuch, D. Vandael, J.S. Lin, O. Selbach, H.L. Haas, O.A. Sergeeva, Excitation of histaminergic tuberomamillary neurons by thyrotropin-releasing hormone, J. Neurosci. 29 (14) (2009) 4471–4483.
[14] O.A. Sergeeva, K. Mazur, A. Kernder, H.L. Haas, R. De Luca, Tachykinins amplify the action of capsaicin on central histaminergic neurons, Peptides 150 (2022) 170729.
[15] H. Yamada, K. Kurokawa, Histochemical studies on endothelin and the endothelin-A receptor in the hypothalamus, J. Cardiovasc Pharm. 31 (1) (1998) S215–218.
[16] M.J. Horwitz, K.D. Bloch, N.B. Kim, J.A. Amico, Expression of the endothelin-1 and oxytocin genes in the hypothalamus of the pregnant rat, Brain Res 648 (1) (1994) 59–64.
[17] K. Kurokawa, H. Yamada, Y. Liu, M. Kudo, Immunohistochemical distribution of the Endothelin-converting enzyme-1 in the rat hypothalamo-pituitary axis, Neurosci. Lett. 284 (1-2) (2000) 81–84.
[18] S. Yamamoto, K. Inenaga, H. Kannan, S. Eto, H. Yamashita, The actions of endothelin on single cells in the anteroventral third ventricular region and supraoptic nucleus in rat hypothalamic slices, J. Neuroendocr. 5 (4) (1993) 427–434.
[19] J.A. Filosa, K. Naskar, G. Perfume, J.A. Iddings, V.C. Biancardi, M.S. Vatta, J. E. Stern, Endothelin-mediated calcium responses in supraoptic nucleus astrocytes influence magnocellular neurosecretory firing activity, J. Neuroendocr. 24 (2) (2012) 378–392.
[20] A. Rancillac, J. Rossier, M. Guille, X.K. Tong, H. Geoffroy, C. Amatore, S. Arbault, E. Hamel, B. Cauli, Glutamatergic control of microvascular tone by distinct GABA neurons in the cerebellum, J. Neurosci. 26 (26) (2006) 6997–7006.
[21] M. Shihara, Y. Hirooka, N. Hori, I. Matsuo, T. Tagawa, S. Suzuki, N. Akaike, A. Takeshita, Endothelin-1 increases the neuronal activity and augments the responses to glutamate in the NTS, ' Am. J. Physiol. 275 (2) (1998) R658–665.
[22] B. Feng, G. Strichartz, Endothelin-1 raises excitability and reduces potassium currents in sensory neurons, Brain Res Bull. 79 (6) (2009) 345–350.
[23] R. Konopkova, I. Vilagi, S. Borbely, H. Kubova, J. Otahal, Effect of Endothelin-1 on the excitability of rat cortical and hippocampal slices in vitro, Physiol. Res 61 (2) (2012) 215–219.
[24] G.M. Drew, C.M. Coussens, W.C. Abraham, Effects of Endothelin-1 on hippocampal synaptic plasticity, Neuroreport 9 (8) (1998) 1827–1830.
[25] M.S. Cembrowski, L. Wang, K. Sugino, B.C. Shields, N. Spruston, Hipposeq: a comprehensive RNA-seq database of gene expression in hippocampal principal neurons, Elife 5 (2016) e14997.
[26] L. Wegmann, H.L. Haas, O.A. Sergeeva, Comparative analysis of adenosine 1 receptor expression and function in hippocampal and hypothalamic neurons, Inflamm. Res 74 (1) (2025) 11.
[27] S. Illes, S. Theiss, H.P. Hartung, M. Siebler, M. Dihne, Niche-dependent development of functional neuronal networks from embryonic stem cell-derived neural populations, BMC Neurosci. 10 (2009) 93.
[28] U.B. Hedrich, C. Liautard, D. Kirschenbaum, M. Pofahl, J. Lavigne, Y. Liu, S. Theiss, J. Slotta, A. Escayg, M. Dihne, H. Beck, M. Mantegazza, H. Lerche, Impaired action potential initiation in GABAergic interneurons causes hyperexcitable networks in an epileptic mouse model carrying a human Na(V)1.1 mutation, J. Neurosci. 34 (45) (2014) 14874–14889.
[29] L.N. Eisenman, C.M. Emnett, J. Mohan, C.F. Zorumski, S. Mennerick, Quantification of bursting and synchrony in cultured hippocampal neurons, J. Neurophysiol. 114 (2) (2015) 1059–1071.
[30] N.J. Michael, J.M. Zigman, K.W. Williams, J.K. Elmquist, Electrophysiological Properties of Genetically Identified Histaminergic Neurons, Neuroscience 444 (2020) 183–195.
[31] R. De Luca, K. Mazur, A. Kernder, T. Suvorava, G. Kojda, H.L. Haas, O.A. Sergeeva, Mechanisms of N-oleoyldopamine activation of central histaminergic neurons, Neuropharmacology 143 (2018) 327–338.
[32] Y. Zhang, G.R. Knutsen, M.D. Brown, L.B. Ruest, Control of Endothelin-a receptor expression by progesterone is enhanced by synergy with Gata2, Mol. Endocrinol. 27 (6) (2013) 892–908.
[33] M.A. Leibl, T. Ota, M.N. Woodward, S.E. Kenny, D.A. Lloyd, C.R. Vaillant, D. H. Edgar, Expression of Endothelin 3 by mesenchymal cells of embryonic mouse caecum, Gut 44 (2) (1999) 246–252.
[34] R. De Luca, T. Suvorava, D. Yang, W. Baumgartel, G. Kojda, H.L. Haas, O. A. Sergeeva, Identification of histaminergic neurons through histamine 3 receptor-mediated autoinhibition, Neuropharmacology 106 (2016) 102–115.
[35] A.P. Davenport, K.A. Hyndman, N. Dhaun, C. Southan, D.E. Kohan, J.S. Pollock, D. M. Pollock, D.J. Webb, J.J. Maguire, Endothelin, Pharm. Rev. 68 (2) (2016) 357–418.
[36] L.E. Mickelsen, W.F. Flynn, K. Springer, L. Wilson, E.J. Beltrami, M. Bolisetty, P. Robson, A.C. Jackson, Cellular taxonomy and spatial organization of the murine ventral posterior hypothalamus, Elife 9 (2020).
[37] P.J. Thul, C. Lindskog, The human protein atlas: a spatial map of the human proteome, Protein Sci. 27 (1) (2018) 233–244.
[38] C.W. Kreipke, C.A. Reynolds, P.C. Schafer, S. Schafer, R. Pirooz, J.A. Rafols, Endothelin receptors A and B are expressed in distinct cellular compartments of rat hippocampus following global ischemia: an immunocytochemical study, Neurol. Res 33 (2) (2011) 162–168.
[39] B. Held, J.M. Pocock, H.A. Pearson, Endothelin-1 inhibits voltage-sensitive Ca2+ channels in cultured rat cerebellar granule neurones via the ET-A receptor, Pflug. Arch. 436 (5) (1998) 766–775.

[40] T.D. Plant, C. Zollner, S.A. Mousa, A. Oksche, Endothelin-1 potentiates capsaicin-induced TRPV1 currents via the Endothelin A receptor, Exp. Biol. Med (Maywood) 231 (6) (2006) 1161–1164.
[41] L. Wu, T.T. Liu, Y. Jin, S. Wei, C.Y. Qiu, W.P. Hu, Endothelin-1 enhances acid-sensing ion channel currents in rat primary sensory neurons, Acta Pharm. Sin. 41 (8) (2020) 1049–1057.
[42] A. Kernder, R. De Luca, Y. Yanovsky, H.L. Haas, O.A. Sergeeva, Acid-sensing hypothalamic neurons controlling arousal, Cell Mol. Neurobiol. 34 (6) (2014) 777–789.
[43] Y. Yanovsky, J.M. Zigman, A. Kernder, A. Bein, I. Sakata, S. Osborne-Lawrence, H. L. Haas, O.A. Sergeeva, Proton- and ammonium-sensing by histaminergic neurons controlling wakefulness, Front Syst. Neurosci. 6 (2012) 23.
[44] L. Walter, N. Stella, Endothelin-1 increases 2-arachidonoyl glycerol (2-AG) production in astrocytes, Glia 44 (1) (2003) 85–90.
[45] G. Cenni, P. Blandina, K. Mackie, D. Nosi, L. Formigli, P. Giannoni, C. Ballini, L. Della Corte, P.F. Mannaioni, M.B. Passani, Differential effect of cannabinoid agonists and endocannabinoids on histamine release from distinct regions of the rat brain, Eur. J. Neurosci. 24 (6) (2006) 1633–1644.
[46] J. Leonova, T. Thorlin, N.D. Aberg, P.S. Eriksson, L. Ronnback, E. Hansson, Endothelin-1 decreases glutamate uptake in primary cultured rat astrocytes, Am. J. Physiol. Cell Physiol. 281 (5) (2001) C1495–1503.
[47] D. Yin, H. Dong, T.X. Wang, Z.Z. Hu, N.N. Cheng, W.M. Qu, Z.L. Huang, Glutamate activates the histaminergic tuberomammillary nucleus and increases wakefulness in rats, Neuroscience 413 (2019) 86–98.
[48] A.A. Mahrous, S.M. Elbasiouny, SK channel inhibition mediates the initiation and amplitude modulation of synchronized burst firing in the spinal cord, J. Neurophysiol. 118 (1) (2017) 161–175.
[49] Z. Niday, B.P. Bean, BK channel regulation of afterpotentials and burst firing in cerebellar purkinje neurons, J. Neurosci. 41 (13) (2021) 2854–2869.
[50] R. Bychkov, J. Glowinski, C. Giaume, Sequential and opposite regulation of two outward K(+) currents by ET-1 in cultured striatal astrocytes, Am. J. Physiol. Cell Physiol. 281 (4) (2001) C1373–1384.
[51] K. Iigaya, H. Onimaru, K. Ikeda, M. Iizuka, M. Izumizaki, Cellular mechanisms of synchronized rhythmic burst generation in the ventromedial hypothalamus, ' Pflug. Arch. 477 (1) (2025) 131–145.
[52] W. Meme, P. Ezan, L. Venance, J. Glowinski, C. Giaume, ATP-induced inhibition of gap junctional communication is enhanced by interleukin-1 beta treatment in cultured astrocytes, Neuroscience 126 (1) (2004) 95–104.
[53] F.C. Barone, M.Y. Globus, W.J. Price, R.F. White, B.L. Storer, G.Z. Feuerstein, R. Busto, E.H. Ohlstein, Endothelin levels increase in rat focal and global ischemia, J. Cereb. Blood Flow. Metab. 14 (2) (1994) 337–342.
[54] Z. Zhou, G. Davar, G. Strichartz, Endothelin-1 (ET-1) selectively enhances the activation gating of slowly inactivating tetrodotoxin-resistant sodium currents in rat sensory neurons: a mechanism for the pain-inducing actions of ET-1, J. Neurosci. 22 (15) (2002) 6325–6330.
[55] P.G. Lysko, N.A. Elshourbagy, M. Pullen, P. Nambi, Developmental expression of Endothelin receptors in cerebellar neurons differentiating in culture, Brain Res Dev. Brain Res 88 (1) (1995) 96–101.
[56] A. Caviedes, M. Varas-Godoy, C. Lafourcade, S. Sandoval, J. Bravo-Alegria, T. Kaehne, A. Massmann, J.P. Figueroa, F. Nualart, U. Wyneken, Endothelial nitric oxide synthase is present in dendritic spines of neurons in primary cultures, Front Cell Neurosci. 11 (2017) 180.
[57] S. Kourembanas, P.A. Marsden, L.P. McQuillan, D.V. Faller, Hypoxia induces Endothelin gene expression and secretion in cultured human endothelium, J. Clin. Invest 88 (3) (1991) 1054–1057.
[58] X. Liu, F. Deng, Z. Yu, Y. Xie, C. Hu, L. Chen, Inhibition of Endothelin A receptor protects brain microvascular endothelial cells against hypoxia-induced injury, Int J. Mol. Med 34 (1) (2014) 313–320.
[59] A.S. Fabricio, G.A. Rae, P. D'Orleans-Juste, G.E. Souza, Endothelin-1 as a central mediator of LPS-induced fever in rats, Brain Res 1066 (1-2) (2005) 92–100.
[60] Y. Kurihara, H. Kurihara, H. Morita, W.H. Cao, G.Y. Ling, M. Kumada, S. Kimura, R. Nagai, Y. Yazaki, T. Kuwaki, Role of Endothelin-1 in stress response in the central nervous system, Am. J. Physiol. Regul. Integr. Comp. Physiol. 279 (2) (2000) R515–521.
[61] G. Perfume, S.L. Nabhen, K.R. Barrera, M.G. Otero, L.G. Bianciotti, M.S. Vatta, Long-term modulation of tyrosine hydroxylase activity and expression by Endothelin-1 and -3 in the rat anterior and posterior hypothalamus, Am. J. Physiol. Regul. Integr. Comp. Physiol. 294 (3) (2008) R905–914.
[62] A.S. Di Nunzio, G. Legaz, V. Rodano, L.G. Bianciotti, M.S. Vatta, Modulatory effect of Endothelin-1 and -3 on neuronal norepinephrine release in the rat posterior hypothalamus, Regul. Pept. 118 (1-2) (2004) 51–59.
[63] D.R. Stevens, A. Kuramasu, K.S. Eriksson, O. Selbach, H.L. Haas, Alpha 2-adrenergic receptor-mediated presynaptic inhibition of GABAergic IPSPs in rat histaminergic neurons, Neuropharmacology 46 (7) (2004) 1018–1022.